



Disruption of mitotic spindle orientation in a yeast dynein mutant

YUN-YING LI*, ELAINE YEH*, TOM HAYS†, AND KERRY BLOOM*

*Department of Biology, 623 Fordham Hall CB# 3280, University of North Carolina at Chapel Hill, Chapel Hill, NC 27599-3280; and †Department of Genetics and Cell Biology, University of Minnesota, St. Paul, MN 55108-1020

Communicated by John Carbon, July 28, 1993 (received for review June 9, 1993)

ABSTRACT Dynein motor isoforms have been implicated as potential kinetochore-associated motors that power chromosome-to-pole movements during mitosis. The recent identification and sequence determination of genes encoding dynein isoforms has now permitted the *in vivo* analysis of dynein function in mitosis. In this report we describe the identification and mutational analysis of the gene, *DHC1*, encoding a dynein heavy chain isoform in *Saccharomyces cerevisiae*. Sequence analysis of a 9-kb genomic fragment of the *DHC1* gene predicts a polypeptide highly homologous to dynein sequences characterized from sea urchin, *Dictyostelium*, *Drosophila*, and rat. Mutations in the yeast dynein gene disrupt the normal movement of the spindle into budding daughter cells but have no apparent effect on spindle assembly, spindle elongation, or chromosome segregation. Our results suggest that, in yeast, a dynein microtubule motor protein has a nonessential role in spindle assembly and chromosome movement but is involved in establishing the proper spindle orientation during cell division.

The major structural and mechanistic features of chromosome segregation on the mitotic spindle appear to be largely conserved between the yeast *Saccharomyces cerevisiae* and higher eukaryotes. Microtubules nucleated by duplicated spindle pole organelles interact with one another and with the sister kinetochores of duplicated chromosomes to establish a bipolar spindle and ensure the equal division of genetic material to opposite spindle poles. The final goal of generating two cells from one involves the mechanism by which the separated chromosomal complements are placed into two separate cells. In this regard, the similarity between yeast and higher eukaryotes is less clear. In yeast, the process of chromosome segregation takes place entirely within the nucleus. The placement of the segregated chromosomal complements, one set of sister chromatids in the mother cell and the other set into the daughter cell, requires the directed movement of the intranuclear spindle into the growing bud of the daughter cell. The site of bud emergence is determined very early in the cell cycle, and bud growth is initiated prior to completion of spindle assembly and chromosome segregation. Movement of the spindle into the bud neck appears to be mediated by the astral microtubule component of the spindle pole body (1). In contrast to the intranuclear microtubules that contribute to spindle assembly, chromosome attachment, and chromosome segregation, the astral microtubules extend from the cytoplasmic face of the spindle pole body and exist in the cytoplasmic milieu.

It is now apparent that a variety of microtubule-associated motor polypeptides are important for the morphogenesis and function of the mitotic spindle in eukaryotes. Substantial progress has been made in analyzing the mitotic contributions of several members of the kinesin superfamily of microtubule motors (2–4). Microtubule motors that are distinct from the kinesins have also been implicated in mitotic spindle function. In particular, previous studies have suggested that the

attachment and/or the movement of chromosomes along spindle microtubules are generated by minus-end motors that reside at or near the kinetochore of chromosomes (5–8). Cytoplasmic isoforms of the microtubule motor dynein are minus-end-directed motors that have been localized to the kinetochore region in mammalian cells and may contribute to chromosome movements in vertebrates. The identification of a dynein gene[‡] from the yeast *S. cerevisiae* provides the opportunity to examine the mitotic function of the dynein polypeptide *in vivo*.

MATERIALS AND METHODS

Isolation of the Yeast Dynein Gene. PCR of the *S. cerevisiae* dynein gene was performed by using degenerate oligonucleotides derived from conserved regions between the sea urchin (9, 10) and *Drosophila* (T.H., unpublished results) dynein sequences. HS-2 (5'-ATHACNCCNCTBACNGAYMG-3') corresponds to amino acid position 1770 (IYT-PLLL) from the coding strand of the *S. cerevisiae* dynein gene and is 2304-fold degenerate. HS-3 (5'-GCNGGHACNGGHAARACNGA-3') corresponds to amino acid position 1798 (AGTGKTE) from the coding strand and is 1152-fold degenerate. HS-4 (5'-CKRTTRAAYTCRTCAARCA-3') corresponds to amino acid 1846 (CFDEFNR) from the noncoding strand and is 128-fold degenerate. HS-5 (5'-GGRTTCATNGTDATRAADAT-3') corresponds to amino acid 1896 (VFITLNP) from the noncoding strand and is 144-fold degenerate. HS-7 (5'-GCYGGHACBGGHARACBGA-3') corresponds to amino acid 1798 (AGTGKTE) from the coding strand and is 324-fold degenerate. For the oligonucleotide sequences N = A, G, T, C; R = A, G; Y = C, T; H = A, T, C; M = A, C; D = G, A, T; K = G, T; B = G, T, C. PCR amplification was performed with 30 cycles using a denaturation time of 90 sec at 94°C, annealing for 2 min at 37°C, and extension at 72°C for 3 min. The 50-μl reaction mixture contained 50 ng of *S. cerevisiae* genomic DNA, each primer at 1.2 μM, and 2.5 units of *Taq* polymerase. The primers HS-2, HS-4, and HS-5 were used for the first round of amplification; 5 μl from the first amplification was used in a second round of amplification with primers HS-3, HS-4, and HS-5. The 171-bp amplified fragment was purified from an agarose gel with GeneClean (Bio 101) and used as a template for a third round of amplification with primers HS-4 and HS-7. A YEp24-based yeast genomic library was screened by colony hybridization using the 171-bp fragment as probe. Candidate plasmids were analyzed by restriction digestion and Southern hybridization. Double-stranded DNA sequence analysis was performed using Sequenase (United States Biochemical).

Construction of Targeted Transformation Vectors. The *dhc1::URA3* disruption deletion vector was constructed by subcloning an internal 3.2-kb *EcoRI DHC1* fragment (containing GKT1, see Fig. 1C Top) into pBR322dH lacking the

The publication costs of this article were defrayed in part by page charge payment. This article must therefore be hereby marked "advertisement" in accordance with 18 U.S.C. §1734 solely to indicate this fact.

Abbreviation: DAPI, 4',6-diamidino-2-phenylindole.

[‡]The sequence reported in this paper has been deposited in the GenBank data base (accession no. L15626).

*Hind*III site. The plasmid was digested with *Hind*II, deleting 254 bp of coding sequence. A 1.1-kb *URA3* fragment was ligated into the *Hind*III site. The *dhc1::URA3* mutation replaced the wild-type *DHC1* gene by one-step gene replacement (11). The plasmid pBR2-1U was digested with *Eco*RI before transformation. Gene replacement at the *DHC1* location was confirmed by Southern hybridization.

The dynein deletion mutation was constructed by first synthesizing the following oligonucleotide primers (5' to 3'): P2, TGTCCATAATGCGAATTCTATAA; P3, GTTACAGCAAGCTTAAGTCAAATA; P4, TGGACGATAA-AAGCTTGAAAGATG; P5, GTGTATGACTGAATTCA-GGGACTA. P2 and P4 contain coding strand DNA corresponding to positions -673 and 6913, respectively. P3 and P5 contain noncoding strand information at positions -235 and 7765, respectively. The primers contain nucleotide substitutions from the *DHC1* sequence to accommodate restriction site insertions (*Eco*RI and *Hind*III) for directional cloning of the amplification products. Plasmid CDF1-1 (YE24 containing the 8.7-kb *Sau*3A *DHC1* sequence) served as template for amplification with primers P2 and P3 or P4 and P5. The two amplification products were purified by GeneClean, digested with *Hind*III, and ligated together. The ligation product was further amplified by PCR with primers P2 and P5. The 1.2-kb amplification product was gel purified and digested with *Eco*RI. This fragment was inserted into pBR322dH. The 1.2-kb *URA3* fragment was subsequently inserted into the *Hind*III site. The plasmid was digested with *Eco*RI to release the *dhc1Δ7::URA3* fragment. This fragment was used for transformation of diploid cells to *Ura*⁺. The resulting diploids have lost DNA from -235 to 6913 bp (7148 bp) relative to the coding sequence. The targeted deletion disruption at the *DHC1* locus in chromosome XI was confirmed by Southern hybridization.

Immunofluorescence and 4',6-Diamidino-2-phenylindole (DAPI) Staining of Wild-Type and Mutant Yeast Cells. Cells were grown to midlogarithmic growth phase and fixed by adding formaldehyde to 4% (wt/vol) and 40 mM potassium phosphate buffer (pH 7.5) directly to the growth medium. Cells were incubated at 25°C for 2 h. Fixed cells were permeabilized with 10% Glusulase (wt/vol) in 1.2 M sorbitol, 40 mM potassium phosphate buffer (pH 7.5), and 25 mM 2-mercaptoethanol at 37°C for 1–2 h. Rat monoclonal anti-yeast α -tubulin antibody, YOL1/34 (1:100) (Accurate Chemicals), and fluorescein-conjugated goat anti-rat IgG antiserum (1:200) (Cappel) were incubated sequentially for 1.5 h at room temperature. For DAPI (Sigma) staining, cells were grown to midlogarithmic growth phase at 32°C in YPD (1% Bacto yeast extract/2% Bacto Peptone/2% dextrose), and aliquots were washed with water and fixed in 70% ethanol at room temperature for 20 min. Fixed cells were washed once with water and stained with DAPI at 1 μ g/ml for 5 min in the dark. The cells were mounted on glass slides as described (12). Cells analyzed at 11°C were grown at 30°C and shifted to 11°C at an OD₆₆₀ = 0.4 for 24 h before fixation and DAPI staining. The cells were examined on a Nikon microscope equipped with epifluorescent optics and photographed on Tri-X Pan 400 film. Greater than 500 cells were counted for each entry in Table 1.

RESULTS AND DISCUSSION

To identify dynein genes in the yeast *S. cerevisiae*, genomic DNA was amplified by PCR using degenerate oligonucleotide primers derived from the predicted amino acid sequence of a sea urchin flagellar (9, 10) and a *Drosophila* cytoplasmic dynein isoform (T.H., unpublished results). Comparison of dynein sequences from sea urchin, *Dictyostelium* (13), and *Drosophila* reveals a highly conserved central domain that contains a cluster of four consensus nucleotide-binding motifs or P loops (GXXGXGKT). Gibbons *et al.* (9) have proposed that the first P loop in this central cluster is the

primary site for ATP hydrolysis. Nested primers flanking this primary ATP hydrolytic site were used to amplify a DNA fragment of 171 bp from yeast genomic DNA. The amplified product was gel purified, radiolabeled, and used to screen a yeast genomic library. A putative yeast dynein clone containing an 8.7-kb genomic insert was purified, and its nucleotide sequence was determined.

The genomic fragment contains the 5' end of the dynein gene, designated *DHC1* (dynein heavy chain), and is illustrated schematically in Fig. 1 A and C. A large open reading frame of 2884 amino acids spans a putative translational initiation methionine and extends toward the C terminus including all four consensus P-loop motifs. In comparison to the cytoplasmic dynein sequences of rat (14), *Dictyostelium*, and *Drosophila*, the yeast dynein shows striking sequence conservation, as well as conservation of the spatial organization of the consensus nucleotide-binding domains (Fig. 1 A and B). In addition to the conserved GXXGXGKT domains (Fig. 1B, boldface and *), identical blocks of 9–12 aa are apparent in neighboring flanking regions (compare yeast to the consensus). In the 1000-aa domain spanning the four consensus P loops, the yeast sequence shows 41–42% amino acid identity and 64–65% similarity to *Dictyostelium*, *Drosophila*, and rat cytoplasmic dynein. In comparison to axonemal dynein isoforms, the degree of sequence conservation is significantly reduced (29% identity and 54% similarity to sea urchin dynein). Analyses of genomic Southern and Northern blots that were probed at high stringency with the 3.2-kb genomic fragment (including the first GKT motif) indicate that the isolated yeast gene is present in a single copy and encodes an \approx 13-kb transcript (data not shown). Taken together the sequence and structural data above confirm that a bona fide dynein-related gene has been identified in the yeast *S. cerevisiae*. We have mapped the yeast dynein, *DHC1*, to chromosome XI by electrophoretic karyotyping and have determined that it lies immediately adjacent to *RNC1* (15), between *TIF1* and *TRK2*. The extensive homology between yeast dynein and the cytoplasmic dynein isoforms characterized from *Drosophila*, *Dictyostelium*, and rat is consistent with the lack of axonemal structures in yeast. The *DHC1* gene encodes a dynein that is presumed to function in cytoplasmic microtubule-based motile processes.

To determine the potential function of *DHC1*, two distinct deletion disruption mutations were constructed *in vitro* within the 8.7-kb genomic DNA fragment (Fig. 1C). The first deletion-disruption mutation, *dhc1::URA3*, was made by inserting a 1.1-kb *Hind*III DNA fragment containing the *URA3* selectable marker gene between a pair of *Hind*III restriction sites located 954 bp upstream from the first P-loop motif (GKT1). The construction results in a deletion of 85 aa from the dynein open reading frame and further disrupts the open reading frame by the insertion of the *URA3* gene. A larger 7.2-kb deletion-disruption construct, *dhc1Δ7::URA3*, was also constructed using specific oligonucleotides as described in *Materials and Methods*. The *dhc1Δ7::URA3* deletion extended from -235 bp to 6913 bp and removed 2305 amino acids from the dynein open reading frame (Fig. 1C). Both mutations were introduced into diploid and haploid cells by fragment-mediated transformation to replace the chromosomal copy of the wild-type dynein gene and were confirmed by Southern hybridization. *Ura*⁺ diploids were recovered and subsequently sporulated and dissected. All four spores were viable, and the *Ura*⁺ marker segregated 2⁺:2⁻. Direct transformation of haploid cells also produced viable *Ura*⁺ progeny and confirmed that the complete *DHC1* coding sequence is not required for cell viability. However, haploid spores or direct transformants containing the *dhc1Δ7::URA3* disruption grew more slowly than wild-type control cells (3 versus 2 h doubling time at 30°C). These results suggest that while dynein is not

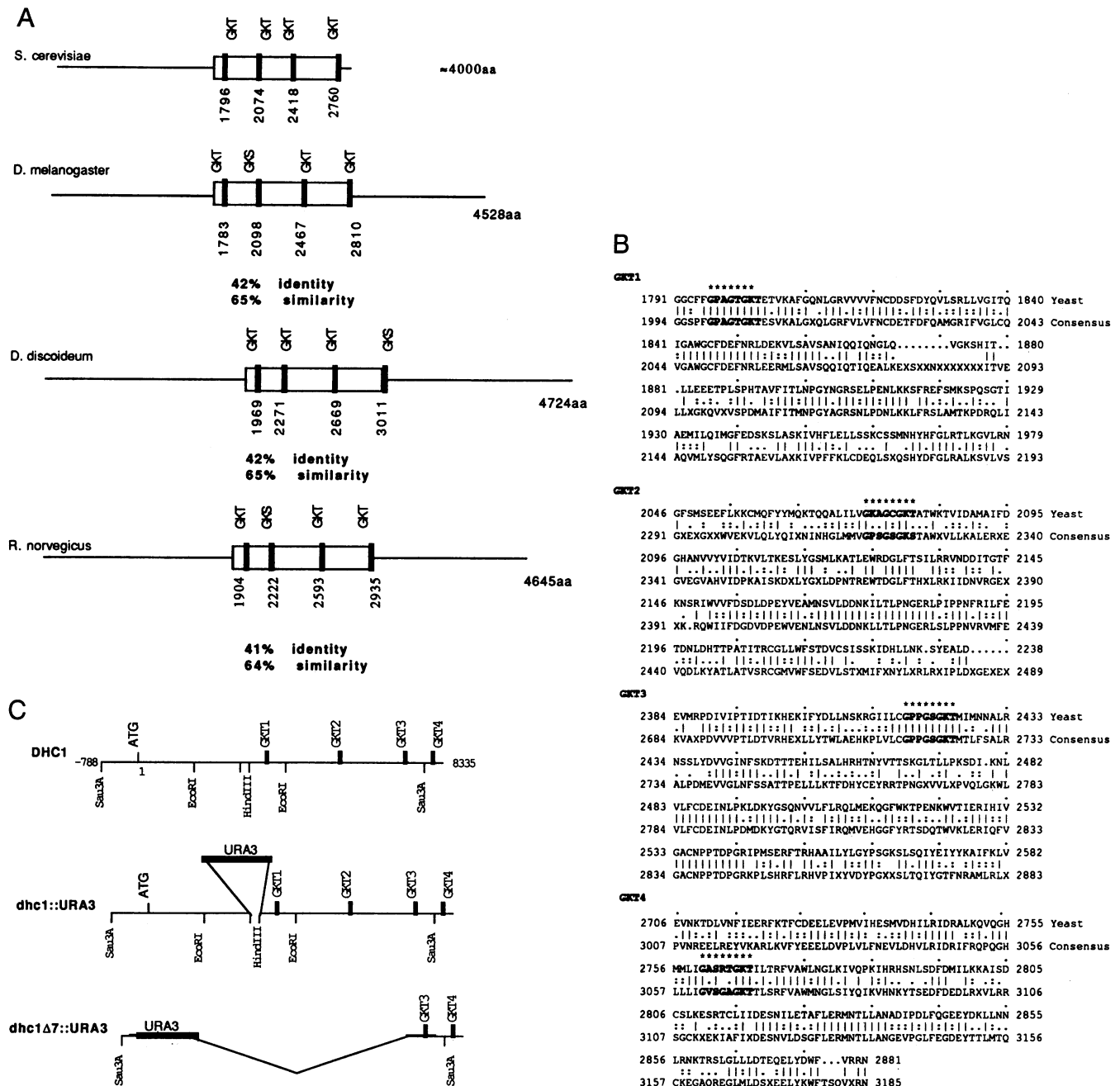


FIG. 1. Sequence organization of yeast, *Drosophila*, *Dictyostelium*, and rat cytoplasmic dyneins. (A) Schematic diagram of the organization of the ATP-binding domains within the dynein sequence of four species. The amino acid positions of the ATP-binding domains (designated by the last three amino acids of the GXXGXGKT motif) are given. The open box denotes the 1000 aa spanning all four ATP-binding regions. Sequence comparison to 1000 aa of yeast are given below each schematic. (B) Deduced amino acid sequence from yeast dynein (Yeast, top line) compared to the consensus sequence from *Dictyostelium*, rat, and *Drosophila* (Consensus, bottom line). One hundred fifty to 200 amino acids surrounding each of the ATP consensus binding sites (GXXGXGKT, boldface and *) are listed. Amino acid identities (I), conservative replacements (:), and nonconservative replacements (.) between the yeast sequence and the consensus sequence are indicated. Periods (.) in the yeast sequence indicate gaps relative to the consensus sequence; X in the consensus sequence denotes gaps relative to the yeast sequence. The numbers indicate the position of the amino acids in the yeast and consensus sequences, respectively. (C) Schematic representation of the wild type and dynein disruption and dynein deletion mutations in yeast chromosome XI. (Top) Linear map of the dynein gene with selected restriction sites and nucleotide binding domains. (Middle) Disruption mutation. The *URA3* gene was inserted at the *HindIII* site deleting 254 bp of dynein coding sequence and disrupting the dynein open reading frame. (Bottom) The deletion mutation was constructed by amplifying DNA (from -235 to -673 and 6913 to 7765) and inserting the *URA3* gene. Seven thousand one hundred forty-eight base pairs of the dynein gene were deleted from the chromosome upon transformation and selection for uracil prototrophs (see *Materials and Methods*).

required for viability, loss of function appears to slow the normal progression of the cell cycle.

To reveal potential cell cycle defects, we examined the nuclear and cell division process in the dynein mutants. The distribution of nuclear DNA and the morphology of mitotic spindles was determined for cells carrying each of the deletion-

disruption mutations. No significant difference was observed between the two deletion-disruption mutants in any of our analyses. The number and size of nuclei were visualized by using the DNA stain DAPI, and mitotic spindle microtubules were visualized by standard immunofluorescence microscopy procedures using a β -tubulin monoclonal antibody (16).

The analysis of DAPI-stained mutant cells in an asynchronous population at 30°C shows that 3–14% of the cells were large, budded cells in which two or more nuclei were located in the larger mother cell and no nuclei were observed in the smaller bud (Table 1). The fraction of bi- and multinucleate cells was significantly increased upon growth at 11°C (14–38%). Mutant cells were followed upon release from α -factor synchrony and examined cytologically. The percentage of bi- and multinucleate cells increased from 1–2% to \approx 15% (data not shown). Thus the binucleate phenotype is dependent upon cell cycle progression. The absence of a concomitant increase in anucleate cells suggests that cells can compensate for the lack of functional dynein. Perhaps the cell cycle pauses until the mitotic spindle adopts the proper position in the budding cell either by a trial and error process or through a second overlapping mechanism.

Examination of spindle morphology in the dynein mutants revealed the primary cause of the multinuclear phenotype. In the large budded cells containing multiple nuclei, mitotic spindles were present only in the mother cell body, with spindle microtubules extending between the separated masses of chromosomal DNA (Fig. 2). Astral microtubules could also be observed extending toward the neck of budding daughter cells (Fig. 2 *B* and *D*). The position of the spindle in these cells reveals the orientation defect. In Fig. 2 *A* and *B*, the spindle is not positioned along the mother–bud axis, whereas in Fig. 2 *C* and *D* axial positioning is correct but chromosomal DNA has segregated in the mother cell. In a few cases, single cells can be observed with two nuclei traversed by the mitotic spindle (Fig. 2 *E* and *F*). Such cells are likely to reflect instances where the cells were unable to compensate for the dynein deficiency prior to cytokinesis. These observations indicate that at the level of the light microscope, the gross features of spindle morphology, spindle assembly, and spindle function (i.e., chromosome segregation to opposite spindle poles) are normal in the dynein mutant cells. However, the loss of dynein function appears to result in the failure of the mitotic spindle to be positioned into the daughter bud. This phenotype is quite distinct from that observed in β -tubulin mutants (*tub2-104* and *tub2-401*), which fail to assemble a spindle at restrictive growth temperature and arrest as large, budded cells with a single nucleus that is retained in the mother cell. In the absence of a functional

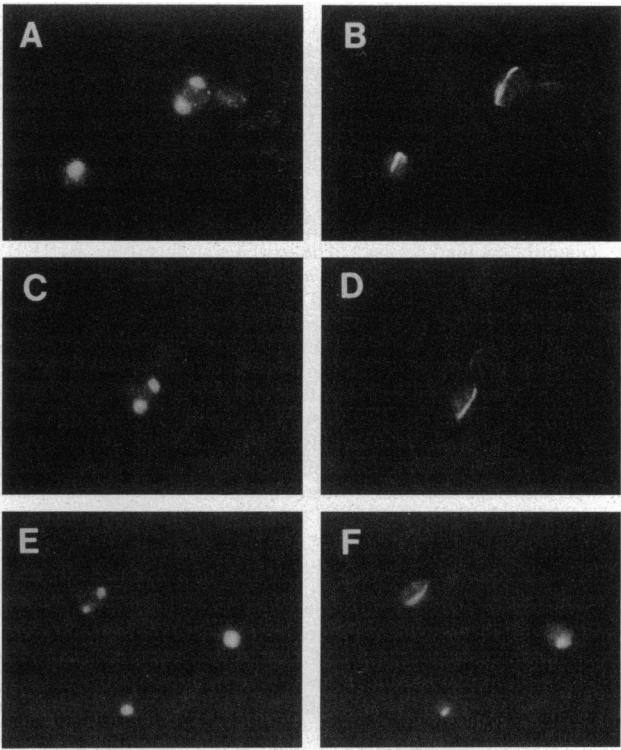









FIG. 2. Microtubule organization in the *dhc1::URA3* cells. Diploid cells homozygous for *dhc1::URA3* were grown at 30°C in YPD. DAPI fluorescence revealed DNA positions (*A*, *C*, and *E*). Immunofluorescence using monoclonal antibodies to tubulin revealed microtubule structures (*B*, *D*, and *F*).

spindle, cells are unable to segregate chromosomes and arrest with duplicated, but unseparated, masses of chromosomal DNA.

Since previous studies have suggested a potential role for dynein motors in chromosome segregation, we extended our analysis to confirm that segregation occurs normally in the yeast dynein mutants as indicated by our microscopic observations. The requirement for dynein in chromosome segregation was examined by determining the mating competency of the mutant cells. Diploid yeast cells are unable to mate, but otherwise diploid cells that have lost one copy of chromosome III containing the *MAT* locus are mating competent. Isogenic *DHC1/DHC1* and *dhc1::URA3/dhc1::URA3* diploids were grown at 30°C and 11°C, and four independent colonies of each strain were mated to appropriate haploid testers to determine mating efficiency (Table 2). There was no significant effect of the *dhc1::URA3* mutation on mating efficiency, even at 11°C, where an elevated number of multinucleate cells and maloriented spindles were observed. However a decrease in nuclear fusion, as observed in *kar* mutants (defective in karyogamy), might decrease the number of mating-competent cells, which would mask an increase in chromosome loss. To address this possibility, the requirement for dynein function in nuclear fusion was examined by cytological inspection of the nucleus after cell fusion during mating. *dhc1::URA3* haploids were able to form zygotes at the same frequency as isogenic wild-type haploids (data not shown). Therefore the quantitative mating data indicate that the *dhc1::URA3* cells are not defective in chromosome segregation *per se*.

The nuclear and spindle phenotype observed in the dynein mutants is reminiscent of recent observations on the phenotype produced by a mutant β -tubulin allele, *tub2-401* (1). At the restrictive temperature of 18°C, cells containing this β -tubulin allele preferentially disassemble astral (cytoplasmic) spindle microtubules and accumulate bi- and multinu-

Table 1. Position of nuclear DNA in dynein mutants

Strain	<i>t</i> , °C	Percentage of cells having nuclear DNA in the position(s) illustrated						
								
		<i>Haploid cells</i>						
<i>DHC1</i>	30	0	23	48	29	0	0	0
	11	0	56	21	23	0	0	0
<i>dhc1::URA3</i>	30	5	43	27	10	2	12	2
	11	7	40	15	4	5	28	2
<i>dhc1::URA3</i>	30	<1	56	23	17	<1	4	<1
	11	5	57	14	5	5	14	<1
<i>dhc1Δ7::URA3</i>	30	<1	62	21	14	<1	3	<1
	11	1	52	21	9	3	13	1
<i>dhc1Δ7::URA3</i>	30	<1	51	27	16	<1	5	<1
	11	7	35	12	6	2	37	1
<i>Diploid cells</i>								
<i>DCH1/DHC1</i>	30	0	45	31	24	0	0	0
	11	0	53	26	31	0	0	0
<i>dhc1::URA3/</i>	30	0.5	40	34	18	0.5	6	1
<i>dhc1::URA3</i>	11	10	33	19	5	5	26	2

Position of nuclear DNA in wild-type and mutant cells. Haploid and diploid cells grown at 30°C and 11°C for 24 h were stained with DAPI, and the position of the DNA was determined by fluorescence microscopy.

Table 2. Mating-competent cells

Tester strain	Observed mating frequency $\times 10^{-5}$			
	30°C*		11°C*	
	MAT α	MAT α	MAT α	MAT α
<i>DHC1/DHC1</i>	7.1 \pm 3.3	2.2 \pm 1.0	4.4 \pm 1.0	2.0 \pm 0.5
<i>dhc1::URA3/</i>				
<i>dhc1::URA3</i>	7.5 \pm 5.7	5.5 \pm 4.8	11.0 \pm 6.6	4.0 \pm 2.5

Quantitative mating assay. The isogenic strains used were KBY5 (α/α *DHC1/DHC1 ura3/ura3 his3/his3 ade1/+ met14/+ leu2/+ +/lys2 +/ade2 +/trp1*) and KBY4 (α/α *dhc1::URA3/dhc1::URA3 ura3/ura3 his3/his3 ade1/+ met14/+ leu2/+ +/lys2 +/ade2 +/trp1*). Diploids and haploid tester strains were grown to midlogarithmic growth phase in YPD, and $\approx 2 \times 10^6$ diploid cells were mixed with $4-8 \times 10^6$ cells of haploid tester strain D562-3C (MAT α *ade6*) or D502-2B (MAT α *ade6*). Appropriate dilutions were made, and the cells were plated onto YPD plates to determine the cell number. The cell mixtures were pelleted briefly, resuspended in 50 μ l of sterile water, and pipetted onto sterile 13-mm nitrocellulose filter discs (Schleicher & Schuell; BA85) on YPD plates. The plates were incubated at 32°C for 3–4 h after which the cells were washed from the discs by vortexing in 1 M sorbitol. The cells were plated onto minimal plates and incubated at 32°C. Only cells that have lost the mating type information on chromosome III, by either chromosome loss, mitotic recombination, or gene conversion will be competent to mate with the tester strain and grow on the appropriate minimal plates. The frequency of these events is tabulated from the number of prototrophs/total cells. Numbers listed are the averages of four independent assays.

*Growth temperature.

create cells as the result of the mitotic spindle remaining in the large mother cell (1). Thus astral microtubules are required for either spindle orientation or nuclear migration into the bud (17, 18). At 11°C, *tub2-401* mutants fail to transport the nucleus to the bud neck, and chromosome segregation is blocked in the absence of a functional spindle. It should be noted that the mutant phenotypes of the dynein deletion disruption and *tub2-401* at 18°C are similar, but distinct. Significantly, the dynein mutants show an apparent delay in cell cycle progression as indicated by the lack of accumulation of anucleate cells (<10%; Table 1). In contrast, 50% of *tub2-401* cells are anucleate after incubation at 18°C and cease cell division after two to three doublings at the restrictive temperature.

As expected, dynein function is dependent upon cellular microtubules. Synthetic lethality was not observed between *dhc1::URA3* and either *tub2-401* or *tub2-104* β -tubulin alleles, and the double mutants exhibit the *tub2* phenotype at restrictive temperature. In addition, the *dhc1::URA3* mutant showed an increased sensitivity to the microtubule depolymerizing drug benomyl (15 μ g/ml). The binucleate phenotype and benomyl sensitivity are observed in a variety of mutants involved in microtubule-dependent processes in the cell (12, 17).

In summary, our present study has identified a gene encoding a yeast dynein that is more homologous in sequence to cytoplasmic dynein isoforms than axonemal dyneins. The analysis of deletion-disruption mutations has shown that the yeast dynein *DHC1* is an active participant in the positioning of the yeast spindle apparatus into the budding daughter cell. The incomplete penetrance of the multinucleate phenotype (3–14% multinucleate cells at 32°C), even in the case of a deletion mutation that removes 2305 amino acids from the

dynein polypeptide, suggests the existence of redundant genes and mechanisms that ensure the spindle is correctly positioned into the growing bud. The mechanism by which the loss of dynein function yields the observed multinucleate phenotype remains to be understood. However, the temperature sensitivity and the β -tubulin dependence of the multinucleate phenotype of the dynein mutations is consistent with a hypothesis in which a yeast dynein anchored in the neck/bud acts upon the astral array of microtubules to pull the spindle apparatus into the bud. Microtubules are not the only cytoskeletal elements involved in spindle positioning. Recently actin has been demonstrated to be required for spindle positioning in the bud (19). Further immunological studies to reveal the location of the dynein isoform should address these and other models and perhaps indicate additional cellular processes, such as vesicular transport and organelle movement, that may utilize the *DHC1* dynein motor. Finally, the failure to observe a dynein mutant phenotype that reflects dysfunction in either spindle assembly, elongation, or chromosome segregation argues against an essential role for dynein in these processes. The existence of redundant motors and mechanisms that mask a "nonessential" mitotic role for dynein remains to be investigated. The present study affords a significant inroad to the further study of dynein motor function.

This work was supported by a grant from the National Institutes of Health (to K.B. and T.H.). T.H. was supported by the Pew Scholars program and the American Chemical Society Junior Faculty Development Award. K.B. was supported by a Research Career Development Award from the National Cancer Institute of the National Institutes of Health.

- Sullivan, D. S. & Huffaker, T. C. (1992) *J. Cell Biol.* **119**, 379–388.
- Hoyt, M. A., He, L., Loo, K. K. & Saunders, W. S. (1992) *J. Cell Biol.* **118**, 109–120.
- Roof, D. M., Meluh, P. B. & Rose, M. D. (1992) *J. Cell Biol.* **109**, 95–108.
- Saunders, W. S. & Hoyt, M. A. (1992) *Cell* **70**, 451–458.
- Pfarr, C. M., Coue, M., Grissom, P. M., Hays, T. S., Porter, M. E. & McIntosh, J. R. (1990) *Nature (London)* **345**, 263–265.
- Steuer, E. R., Wordeman, L., Schorer, T. A. & Sheetz, M. P. (1990) *Nature (London)* **345**, 266–268.
- Wordeman, L., Steuer, E. R., Sheetz, M. P. & Mitchison, T. (1991) *J. Cell Biol.* **114**, 285–294.
- Hyman, A. A., Middleton, K., Centola, M., Mitchison, T. J. & Carbon, J. (1992) *Nature (London)* **359**, 533–536.
- Gibbons, I. R., Gibbons, B. H., Moczek, G. & Asai, D. J. (1991) *Nature (London)* **352**, 640–643.
- Ogawa, K. (1991) *Nature (London)* **352**, 643–645.
- Rothstein, R. J. (1983) *Methods Enzymol.* **101**, 202–211.
- Berlin, V., Styles, C. A. & Fink, G. R. (1990) *J. Cell Biol.* **111**, 2573–2586.
- Koonce, M. P., Grissom, P. M. & McIntosh, J. R. (1992) *J. Cell Biol.* **119**, 1597–1604.
- Mikami, A., Paschal, B. M., Mazumdar, M. & Vallee, R. B. (1993) *Neuron* **10**, 787–796.
- Chow, T. Y.-K., Perkins, E. L. & Resnick, M. A. (1992) *Nucleic Acids Res.* **20**, 5215–5221.
- Adams, A. E. & Pringle, J. R. (1984) *J. Cell Biol.* **98**, 934–945.
- Huffaker, T. C., Thomas, J. H. & Botstein, D. (1988) *J. Cell Biol.* **106**, 1997–2010.
- Jacobs, C. W., Adams, A. E., Szaniszló, P. J. & Pringle, J. R. (1988) *J. Cell Biol.* **107**, 1409–1426.
- Palmer, R. E., Sullivan, D. S., Huffaker, T. C. & Koshland, D. (1992) *J. Cell Biol.* **119**, 583–593.